HHS Public Access
Author manuscript
Exp Neurol. Author manuscript; available in PMC 2020 October 01.

Published in final edited form as:
Exp Neurol. 2019 October ; 320: 112959. doi:10.1016/j.expneurol.2019.112959.

In vivo glutamate clearance defects in a mouse model of Lafora disease

C. Muñoz-Ballester[1,#], **N. Santana**[2,#], **E. Perez-Jimenez**[1], **R. Viana**[1], **F. Artigas**[2,4,5], **P. Sanz**[1,3,*]

[1]IBV-CSIC. Instituto de Biomedicina de Valencia, Consejo Superior de Investigaciones Científicas, Valencia, Spain.

[2]Department of Neurochemistry and Neuropharmacology, Institut d'Investigacions Biomédiques de Barcelona , CSIC, Barcelona, Spain.

[3]CIBERER. Centro de Investigación Biomédica en Red de Enfermedades Raras, (group U742) Valencia, Spain

[4]Instituto de Investigaciones Biomédicas August Pi i Sunyer (IDIBAPS), Barcelona, Spain

[5]CIBERSAM. Centro Investigación Biomédica en Red de Salud Mental, Barcelona, Spain

Abstract

Lafora disease (LD) is a fatal rare neurodegenerative disorder characterized by epilepsy, neurodegeneration and insoluble polyglucosan accumulation in brain and other peripheral tissues. Although in the last two decades we have increased our knowledge on the molecular basis underlying the pathophysiology of LD, only a small part of the research in LD has paid attention to the mechanisms triggering one of the most lethal features of the disease: epilepsy. Recent studies in our laboratory suggested that a dysfunction in the activity of the mouse astrocytic glutamate transporter 1 (GLT-1) could contribute to epilepsy in LD. In this work, we present new *in vivo* evidence of a GLT-1 dysfunction, contributing to increased levels of extracellular glutamate in the hippocampus of a mouse model of Lafora disease (*Epm2b−/−*, lacking the E3-ubiquitin ligase malin). According to our results, *Epm2b−/−* mice showed an increased neuronal activity, as assessed by *c-fos* expression, in the hippocampus, an area directly correlated to epileptogenesis. This brain area presented lesser ability to remove synaptic glutamate after local GLT-1 blockade with dihydrokainate (DHK), in comparison to *Epm2b+/+* animals, suggesting that these animals have a compromised glutamate clearance when a challenging condition was presented. These results correlate with a hippocampal upregulation of the minor isoform of the *Glt-1* gene, named *Glt-1b*, which has been associated with compensatory mechanisms activated in

[*]**Corresponding author**: Dr. Pascual Sanz, Instituto de Biomedicina de Valencia, CSIC and Centro de Investigación Biomédica en Red de Enfermedades Raras (CIBERER), Jaime Roig 11, 46010-Valencia, Spain. Tel. +34963391779, FAX. +34963690800, sanz@ibv.csic.es.
[#]These authors contributed equally to this work.

Conflict of interest: On behalf of all authors, the corresponding author states that there is no conflict of interest.

response to neuronal stress. In conclusion, the hippocampus of *Epm2b−/−*mice presents an *in vivo* impairment in glutamate uptake which could contribute to epileptogenesis.

Keywords

Lafora disease; glutamate transport; c-fos; GLT-1; epileptogenesis

INTRODUCTION

Lafora progressive myoclonus epilepsy (Lafora disease, LD, OMIM 254780) is a fatal rare autosomal recessive neurodegenerative disorder characterized by epilepsy, neurodegeneration and the accumulation of insoluble polyglucosan inclusions, known as Lafora bodies, in the cytoplasm of neurons, astrocytes and other cells in peripheral tissues [(Turnbull et al., 2016), (Rubio-Villena et al., 2018)]. The first clinical signs of the disease appear in the late childhood or the adolescence, having a rapid progression characterized by dementia and a worsening of the seizures that lead to the death of the patient ten years after the onset of the disease (Turnbull et al., 2016). At present, no treatment for this disorder is available and the molecular bases underlying this disease are still far from being understood. In the last decades, many groups have contributed to clarify some of the molecular processes implicated in the pathophysiology of LD. Mutations in two genes, *EPM2A* [(Minassian et al., 1998), (Serratosa et al., 1999)] and *EPM2B* (Chan et al., 2003), were identified which explained 92% of the human cases. *EPM2A* encodes laforin, a dual specific phosphatase (Minassian et al., 2000), and *EPM2B* encodes malin, an E3-ubiquitin ligase (Chan et al., 2003). Both proteins form a functional complex involved in many cellular pathways including glycogen metabolism, protein clearance or oxidative stress, and defects in the function of this complex could explain in part the neurodegeneration and the presence of Lafora bodies observed in patients. However, the molecular basis of the feature that limits daily life of patients, namely epilepsy, is still poorly known.

The only mechanism proposed to explain epilepsy in LD focuses on the dysfunction of inhibitory GABAergic neurons [(Sharma et al., 2013), (Ortolano et al., 2014)]. However, none of the anti-epileptic treatments targeting neurons have worked in LD until now. Recent studies in our group highlighted the importance that astrocytes could have in the development of this pathology (Rubio-Villena et al., 2018). These cells play multiple roles in the maintenance of brain homeostasis. In addition, they have also been described as possible drivers of epilepsy (Robel et al., 2015). One of the multiple functions that astrocytes perform in the brain is to eliminate the excess of glutamate from the synaptic cleft. Glutamate is the main excitatory neurotransmitter participating in 70% of the excitatory synapses [(Tanaka et al., 1997), (Petr et al., 2015), (Danbolt et al., 2016a)]. Its removal from the extracellular space is essential to avoid a hyperexcitation that could lead to seizures or even to neuronal death by excitotoxicity [(Olney et al., 1972), (Olney et al., 1986), (Meldrum, 1986), (Meldrum, 1991), (Choi and Hartley, 1993), (Murphy-Royal et al., 2017)]. To this purpose, astrocytes express high affinity glutamate transporters in their processes which remove the excess of glutamate present in the synaptic cleft (Murphy-Royal et al., 2017).

In mouse, there are five glutamate transporters expressed in the central nervous system: glutamate transporter 1 (GLT-1) [(Danbolt et al., 1990), (Arriza et al., 1994)], glutamate aspartate transporter (GLAST) [(Storck et al., 1992), (Arriza et al., 1994)], excitatory aminoacid carrier 1 (EAAC1) [(Kanai and Hediger, 1992), (Arriza et al., 1994)], excitatory aminoacid transporter 4 (EAAT4) (Fairman et al., 1995) and excitatory aminoacid transporter 5 (EAAT5) (Arriza et al., 1997). GLT-1 and GLAST are mostly expressed in astrocytes, GLT-1 being responsible for the clearance of 90% of the synaptic glutamate (Tanaka et al., 1997). Deficiencies in GLT-1 function have been associated with epilepsy [(Tanaka et al., 1997), (Coulter and Eid, 2012)]. In fact, *Glt-1* KO mice die soon after birth due to uncontrolled seizures (Tanaka et al., 1997). Recent studies in our group described an abnormal subcellular location of GLT-1 in primary astrocytes from mouse models of Lafora disease (*Epm2a−/−* and *Epm2b−/−*), which showed decreased glutamate uptake activity (Munoz-Ballester et al., 2016). However, our study did not explain whether these findings had consequences at the level of the *in vivo* glutamate homeostasis.

In this work, we first mapped the brain areas with a higher neuronal activity that could be involved in epileptogenesis in LD and then analyzed by microdialysis the ability of the selected areas to clear up the extracellular glutamate after artificially inducing an excitatory challenge. The two inputs used were the local administration of dihydrokainate (DHK), a GLT-1 inhibitor, and a subconvulsive dose of pentylenetetrazol (PTZ), an epileptogenic drug that inhibits the GABAergic inhibitory system and increases the excitation/inhibition ratio. Our results demonstrate that in *Epm2b−/−* mice glutamate uptake is compromised when we administered dihydrokainate as an excitatory challenge, suggesting an *in vivo* dysfunction of GLT-1 in the process. In addition, in the presence of PTZ, we also observed a tendency to increased levels of glutamate.

This work, therefore, presents new evidence for the implication of astrocytes in the pathophysiology of LD, emphasizing the relevance of GLT-1 dysfunction in the loss of glutamate homeostasis in the brain of LD animal models.

MATERIAL AND METHODS.

Ethic statement, animal care, mice and husbandry.

This study was carried out in strict accordance with the recommendations in the Guide for the Care and Use of Laboratory Animals of the Consejo Superior de Investigaciones Cientificas (CSIC, Spain). All mouse procedures were approved by the animal committee of the Instituto de Biomedicina de Valencia-CSIC [Permit Number: INTRA12 (IBV-4)]. All efforts were made to minimize animal suffering. To eliminate the effect of differences in the genetic background of the animals, we backcrossed the previously described *Epm2b−/−* mice (with a mixed background 129sv:C57BL/6) [(Aguado et al., 2010), (Criado et al., 2012)] with control C57BL/6JRccHsd mice obtained from Harlan laboratories (Barcelona, Spain) ten times to obtain homozygous *Epm2b−/−*in a pure background. Mice were maintained in the IBV-CSIC facility on a 12/12 light/dark cycle under constant temperature (23°C) with food and water provided *ad libitum*.

c-*fos* analysis by *in situ* hybridization.

The expression of *c-fos* mRNA using *in situ* hybridization was performed as previously described (Kargieman et al., 2007). Mice were sacrificed by cervical dislocation. The brains were rapidly removed, frozen on dry ice, and stored at −20°C. Brain tissue sections, 14 μm thick, were cut using a microtome-cryostat (Microm HM500 OM, Walldorf, Germany), thaw mounted onto APTS (3-aminopropyltriethoxysilane, Sigma, St Louis, MO)-coated slides and kept at −20°C until analysis. The oligodeoxyribonucleotide probes used were as previously described in (Kargieman et al., 2007). Probes were synthesized on a 380 Applied Biosystems DNA synthesizer (Applied Biosystems, Foster City, CA). *c-fos* oligonucleotide was labeled at its 3'-end with [^{33}P]-dATP (>3000 Ci/mmol; DuPont-NEN, Boston, MA) with terminal deoxynucleotidyltransferase (TdT, Calbiochem, La Jolla, CA) and purified with ProbeQuant G-50 Micro Columns (GE Healthcare UK Limited, Buckinghamshire, UK). Analysis of brain sections was performed in an Olympus BX51 Stereo Microscope equipped with an Olympus Microscope Digital Camera DP71, with the aid of Visiopharm Integrator System software (Olympus).

In vivo microdialysis procedure

Concentric microdialysis probes were constructed with a 2-mm-long membrane. Following anesthesia with sodium pentobarbital (120 mg/kg i.p.), 9-month-old male mice were placed in a stereotaxic frame (David Kopf Instruments, Tujunga, CA, USA), dialysis probes were implanted in the hippocampus and secured to the skull with anchor screws and dental cement. Stereotaxic coordinates from Bregma and skull surface were: AP −3.00 mm, L −3.00 mm, DV −4.5 mm; according to Franklin and Paxinos (Franklin, 2012). Microdialysis experiments were conducted 20–24 h after surgery in freely moving mice by continuously perfusing probes with an artificial cerebrospinal fluid (aCSF) containing 125 mM NaCl, 2.5 mM KCl. The aCSF was perfused at 1.6 μL/min with a Harvard model 22 syringe pump (Harvard Apparatus, South Natick, MA, USA) attached to an overhead liquid swivel (Instech, Plymouth Meeting, PA, USA). An initial sample of dialysate corresponding to the first 2.5 h was discarded and then, one sample of aCSF (16 μL) was collected every 10 minutes up to 3 samples, to establish a stable baseline level of glutamate before any pharmacological intervention. Next, dihydrokainate (DHK) was administered locally by reverse dialysis through the dialysis probes. We administered 0.1 mM, 0.3 mM, 1 mM and 3 mM doses and we collected one sample of dialysate every 10 minutes (4 samples for each DHK dose).

On the following day, mice were injected intraperitoneally with the pro-convulsive agent pentylenetetrazol (PTZ) in order to examine glutamate levels in a challenging condition involving an increase of the excitation/inhibition ratio. After a 2.5 h stabilization period, 4 baseline dialysate 10 min samples were collected before PTZ treatment (10 and 30 mg/kg i.p.). A total of six samples of dialysate per dose were collected.

At the completion of dialysis experiments, mice were sacrificed by cervical dislocation and brains were rapidly removed and frozen in dry ice for subsequent histological examination.

Biochemical determinations

The concentration of glutamate (Glu) in dialysate samples was determined by an HPLC system consisting of a Waters 717 plus auto-sampler, a Waters 600 quaternary gradient pump, and a Nucleosil 5μm particle size ODS column (10 × 0.4 cm; Tekno-kroma, Spain). Dialysate samples were precolumn-derivatized with OPA reagent and the entire process was carried out by the autosampler. Briefly, 90 μL distilled water was added to 10 μL of dialysate sample and this was followed by the addition of 15 μL OPA reagent. After 2.5 min reaction, 80 μL of this mixture was injected into the column. Detection was carried out with a Waters 470 scanning fluorescence detector using excitation and emission wavelengths of 360 nm and 450 nm, respectively. The mobile phase was pumped at 0.8 μL/min and consisted of two components: solution A, made up of 0.05 M Na_2HPO_4, 28% methanol, adjusted to pH 6.4 with 85% H_3PO_4, and solution B, made up of 100% methanol/H_2O (8:2 ratio) (Calcagno et al., 2006). After the elution of glutamate peak at 3 min with 100% solution A, a gradient was established going from 100% solution A to 100% solution B in 2 min. After washing out late-eluting peaks (3 min), mobile phase returned to initial conditions (100% solution A) in 2 min. The detection limit for glutamate was 0.2 pmol (signal-to-noise ratio 3). Quantification of glutamate was carried out by comparison to a daily standard curve comprising the concentrations of neurotransmitters expected in dialysate samples.

mRNA quantification by qPCR.

Sixteen-days-, three-month- and twelve-month-old *Epm2b+/+* and *Epm2b−/−* mice were sacrificed by cervical dislocation. Brain was recovered and the hippocampus was dissected from the left hemisphere, snip-frozen in liquid nitrogen and stored at −80°C. Hippocampi were lysed in 400 μL trizol (TriPure Isolation Reagent, Sigma) on ice, incubated 10 min at room temperature and 80 μL of chloroform were added. Samples were vigorously vortexed and incubated at room temperature for 10 minutes. Samples were spun at 12,000 x g 15 minutes at 4°C and 150 μL of the upper phase were collected. 187 μL of isopropanol were added and the samples were vigorously vortexed, incubated for ten minutes and spun at 16,000 x g for 30 minutes at 4°C. The supernatant was discarded and the pellet was washed with 70% ethanol (v/v), vigorously vortexed and centrifuged again at 16,000 x g for 5 minutes at 4°C. The pellet was dried, resuspended in 50 μL of nuclease-free water and incubated at 55°C for 15 minutes. The RNA concentration was determined using a NanoDrop 2000 (Thermo Scientific, Madrid, Spain).

Reverse transcription was carried out with the Expand Reverse Transcriptase kit (Roche, Barcelona, Spain) from 1 μg of RNA according to manufacturer's instructions. From the resultant cDNA, a 1:5 dilution was used in the qPCR assay. The qPCR assay was based in the Universal Probes system (Roche, Barcelona, Spain) combined with the primers indicated by Roche Probe Finder sofware (Table I). The amplification reagent used was the TaqMan Fast Universal Master Mix (Applied Biosystems, Madrid, Spain), the thermocycler was the 7500 Real-Time PCR System (Applied Biosystems, Madrid, Spain) and the concentration and programs used were those indicated by the manufacturer. The quantification method used was the ΔΔCt, using as reference the expression of the hipoxantine-guanine phophoribosyltransferase (*Hprt*) housekeeping gene.

Immunohistochemistry analyses.

Twelve-month-old mice were sacrificed by cervical dislocation. Brain was recovered and the right hemisphere was fixed in 4% paraformaldehyde in phosphate buffer saline (PBS) for 24 hours at 4°C. After three washes with PBS, the samples were dehydrated and embedded in paraffin and sectioned at 4 μm using a microtome HM-340E (Microm, Madrid, Spain). Sections were deparaffinized, rehydrated, and endogenous peroxidase was inactivated by incubating 20 min with a mixture of MetOH/H_2O_2 (29:1). Heat induced epitope retrieval was next performed incubating at 95°C for 10 min in 10 mM EDTA Tris-HCl pH9.0 buffer. Sections were next blocked in blocking buffer [5% fetal bovine serum (FBS)/1% bovine serum albumin (BSA), in PBS] and incubated overnight at 4°C with the primary antibody. After three washes of 10 min in PBS, sections were incubated for one hour at room temperature with the biotinylated secondary antibody, washed three times with PBS for 5 min, incubated with the ABC kit (ABC, Vectastain Elite, Vector Laboratories, Madrid, Spain) for 30 min in the dark, washed three times in PBS for 5 min and developed using metal enhanced DAB method (DAB, Vector Laboratories, Madrid, Spain). IHC sections were finally counterstained with haematoxylin (Sigma, Madrid, Spain), dehydrated and mounted in DPX (Merck, Germany). Images were acquired with a DM6000 Leica Microscope and analyzed with Image J software (NIH, Bethesda, MD, USA). As primary antibodies we used guinea pig against GLT-1 (#AB1783, Millipore), rabbit against EAAT1 (GLAST) (#sc-15316, Santa Cruz) and rabbit against EAAT3 (EAAC1) (#124802, Abcam). As secondary antibodies we used goat against rabbit (#711065152, Jackson ImmunoResearch) or guinea pig (#AP-108B, Millipore) conjugated with biotin.

Western blot analyses

Mouse hippocampal homogenates were lysed in sodium phosphate buffer (pH 7.4) containing 1% SDS and 1mM PMSF, as suggested (Danbolt et al., 2016b). The homogenates were passed five times through 25 gauge needle in 1 ml syringe, vortexed for 40 seconds, boiled 5 min at 95°C and centrifuged at 12,000xg for 10 min. Supernatants were collected, subjected to SDS-PAGE, transferred into PVDF membrane and revealed with the appropriate antibodies: guinea pig anti-GLT-1, rabbit against EAAT1 (GLAST) and rabbit against EAAT3 (EAAC1) (see above). Mouse anti-Gapdh (sc-32233, Santa Cruz Biotechnologies) was used as loading control. Primary antibodies were incubated overnight at 4°C. Images were obtained with a FujiLAS4000 using Lumilight Western Blotting Substrate (Roche). The results were analysed using the software Image Studio version 5.2 (LI-COR Biosciences, Germany). Experiments were performed in four individuals from each genotype.

Statistical analysis.

Animals were distributed randomly into experimental groups. Two-way ANOVA plus Bonferroni post-hoc tests or *t*-tests were used to examine the effect of genotype and/or treatment, as appropriate. Statistical analysis was performed using GraphPad Prism 7 (GraphPad Software). Unless stated otherwise, all values are reported as mean ± SD. In microdialysis experiments, area under the curve (AUC) values of selected time periods have also been used when indicated. The significance level was set to p≤0.05. Statistical significance is indicated with *p≤0.05, **p≤ 0.01, ***p≤ 0.001, **** p≤ 0.0001.

RESULTS

Epm2b−/− mice show higher basal *c-fos* expression in a CA1-CA3 region of the hippocampus than *Epm2b+/+* mice.

To identify brain areas with a putatively altered neuronal activity, we performed histological studies examining the basal expression of the early gene *c-fos*, a well-established marker of neuronal activation ((Sagar et al., 1988), (Herrera and Robertson, 1996)), using *in situ* hybridization. Coronal brain slices from 9-month-old *Epm2b+/+* and *Epm2b−/−* animals were used. *c-fos* expression was analyzed in several areas of the brain, according to Franklin and Paxinos (Franklin, 2012): prefrontal cortex (AP +2.1 mPFC), orbital cortex (AP +2.1 ORB), somatosensory cortex (AP −2.00), hippocampus (both dentate gyrus and CA1-CA3 regions) (AP −2.00), cortex (AP −3.00), and hippocampus (both dentate gyrus and CA1-CA3 regions) (AP-3.00). A statistically significant and regionally-selective increase in *c-fos* expression in *Epm2b−/−* mice -as compared to *Epm2b+/+* mice- was found in the CA1-CA3 region of the hippocampus (AP −3.00) (Fig. 1). For this reason, subsequent studies were performed in this hippocampal formation. On the other hand, a significant decrease in c-*fos* expression was found in somatosensory cortex (AP −2.00) (Fig. 1).

Glutamate clearance is impaired in *Epm2b−/−* mice after DHK administration.

Previous studies in our laboratory suggested a dysregulation in GLT-1 function as a mechanism contributing to epileptogenesis in LD (Munoz-Ballester et al., 2016). Since we found that hippocampal CA1-CA3 areas were potential regions of increased neuronal activity (see above), we performed microdialysis experiments in this area, in order to determine the glutamate clearance status. Probes were implanted in the hippocampus of 9-month-old *Epm2b+/+* and *Epm2b−/−* mice. After collecting basal dialysate fractions, the selective GLT-1 inhibitor dihydrokainate (DHK) was locally applied by reverse dialysis at increasing concentrations (0.1, 0.3, 1 and 3 mM). DHK elevated extracellular glutamate levels in a concentration- and genotype-dependent manner (two-way ANOVA plus Bonferroni post-hoc test, p<0.0001 treatment factor; p<0.05 genotype factor) with a greater elevation in *Epm2b−/−* mice, particularly at 1 mM DHK (Fig. 2A).

Hippocampal glutamate clearance in *Epm2b−/−* mice after PTZ administration.

We were also interested in determining whether under epileptogenic conditions, the hippocampal formation was also able to remove the excess of glutamate that could be potentially released. With this aim, we injected intraperitoneally pentylenetetrazole (PTZ), an epileptogenic drug, in 9-month-old *Epm2b+/+* or *Epm2b−/−* mice and we determined the levels of extracellular glutamate in the hippocampus. We used doses that had been previously described as sufficient to induce seizures in *Epm2b−/−* mice but not in *Epm2b+/+* (10 mg/kg and 30 mg/kg) (Garcia-Cabrero et al., 2014). It was reasoned that any potential impairment in GLT-1 function would lead to a defective clearance of extracellular glutamate after the increase in excitatory neurotransmission induced by PTZ.

Overall, PTZ evoked a higher elevation of extracellular glutamate in *Epm2b−/−* mice than in *Epm2b+/+* mice (Fig. 2B). However, these differences did not reach statistical significance (two-way ANOVA) when analyses were performed with the individual values of each dialysate fraction, likely due to the large deviation of glutamate values. However, the overall effect, as assessed by AUC (area under the curve) values, revealed a greater effect of PTZ in *Epm2b−/−* mice ($p<0.05$, multiple *t*-test) at the 10 mg/kg dose (Fig. 2C).

Glt-1b **mRNA levels are upregulated in hippocampus of** ***Epm2b−/−*** **adult mice.**

Since, as described above, we observed a deficiency in glutamate uptake in *Epm2b−/−* mice when DHK was administered, we wanted to understand the molecular basis underlying this process. To accomplish this, we first determined by qPCR the mRNA levels of *Glt-1a* and *Glt-1b*, the two most common isoforms of the glutamate transporter *Glt-1*, in the hippocampus of 16-days-, 3-month- and 12-month-old *Epm2b+/+* and *Epm2b−/−* animals. We also checked the mRNA expression of the other main glutamate transporters present in the brain, *Glast* and *Eaac1*, to dismiss a possible compensation of *Glt-1* by these other transporters. Our results showed an increase in *Glt-1b* expression in *Epm2b−/−* animals of 12 months of age compared to *Epm2b+/+*, but no differences were observed at any other age (Fig. 3B). In addition, our results indicated that there were no differences in the expression of the *Glt-1a* isoform or *Glast* between *Epm2b+/+* and *Epm2b−/−* at any age (Fig. 3A, 3C). In the case of *Eaac1*, we observed a significant decrease in gene expression in *Epm2b−/−* mice at 12 months of age in comparison to control mice, but there were no differences at 16 days or three months of age between the two genotypes (Fig. 3D). These results suggested a major change in the expression of *Glt-1b* and a decrease in the expression of *Eaac1* in old *Epm2b−/−* mice but no changes in the expression of the other glutamate transporters in comparison to control animals.

GLT-1 protein expression is not altered in the hippocampus of ***Epm2b−/−*** **mice.**

After detecting an upregulation in *Glt-1b* mRNA levels in *Epm2b−/−* mice compared to *Epm2b+/+*, we decided to study the protein levels of GLT-1 in the hippocampus of *Epm2b−/−* mice of 12-months of age. With this aim, we performed immunohistochemistry analyses in paraffinized brain slices of *Epm2b+/+* and *Epm2b−/−* mice using appropriate antibodies. For this experiment we had to use an antibody that recognizes both the GLT-1a and the GLT-1b isoforms, as we could not find any commercial isoform-specific antibody. As shown in Fig. 4A, we did not find differences in GLT-1 protein levels in the hippocampus of *Epm2b+/+* and *Epm2b−/−* mice. Similar results were obtained when we analyzed GLT-1 protein levels by Western blot (Fig. 4D) This was not surprising since we had previously indicated that the total levels of GLT-1, assessed by Western blot, were similar in astrocytes from control and *Epm2b−/−* mice (Munoz-Ballester et al., 2016).

We also studied the protein levels of GLAST and EAAC1, the two other glutamate transporters present in the hippocampus (Fig. 4B, 4C and 4D). Again, we could not find any differences in GLAST or EAAC1 protein levels in the hippocampus of 12-month-old *Epm2b+/+* and *Epm2b−/−*mice.

DISCUSSION

In recent years, many studies have contributed to the understanding of the molecular basis underlying the pathophysiology of LD. However, only a small part of these studies has focused on the mechanisms contributing to the epileptogenesis in this fatal disease. Previous studies in our group suggested the implication of GLT-1 and astrocytes in the underlying cause of epilepsy in LD [(Munoz-Ballester et al., 2016), (Rubio-Villena et al., 2018)]. Indeed, astrocytes are emerging as key players in synaptic function, controlling the extracellular levels of ions and neurotransmitters, responding to them and regulating synaptic transmission and plasticity [(Perea and Araque, 2007), (Perea et al., 2014)]. Accordingly, astrocytes play important roles in animal behavior, being involved in the processing of sensory, cognitive, emotional and motor information [(Oliveira et al., 2015), (Cho et al., 2018), (Brancaccio et al., 2019)]. In particular, astroglial glutamate transporters GLT-1 and GLAST are responsible for the reuptake of most synaptic glutamate from central excitatory synapses [(Danbolt et al., 1992), (Petr et al., 2015)], thereby directly controlling neuronal excitability.

The present results confirmed these previous notions and indicate that *Epm2b−/−*mice show an impaired glutamate clearance, in parallel with an increased *c-fos* expression in the hippocampal formation. The latter variable has been used as a surrogate marker of neuronal function, as indicated by previous studies [(Sagar et al., 1988), (Dragunow and Faull, 1989), (Herrera and Robertson, 1996), (Konkle and Bielajew, 2004)] and, although the final proof would be to perform electrophysiological measurements (e.g., EEG to detect seizures), the expression of *c-fos* has been widely used to map seizure-activity in the brain [(Hirsch et al., 1997), (Andre et al., 1998), (Ferland et al., 1998), (Klein et al., 2004), (Kadiyala et al., 2015)]. Likewise, changes in c-*fos* expression suing the present *in situ* hybridization method have always paralleled the changes in excitatory neuron discharge when examined [(Kargieman et al., 2007), (Santana et al., 2011), (Llado-Pelfort et al., 2012)]. As far as we know, this is the first time that a specific area of the brain in a LD mouse model has been associated with an increase in neuronal activity without any pharmacological intervention. Therefore, our results suggest that there is a characteristic pattern of an excess of neuronal activity in the hippocampus of these animals under basal conditions. Given the involvement of the hippocampal formation in seizure activity, it is likely that the higher neuronal activity in this brain area may account for the greater seizure susceptibility of *Epm2b−/−* mice.

On the other hand, the present microdialysis data support our previous observations on the presence of a dysfunctional GLT-1 transporter in *Epm2b−/−* mice (Munoz-Ballester et al., 2016). Hence, the local blockade of GLT-1 with DHK, applied by reverse dialysis, elevated extracellular glutamate levels in mouse hippocampus in a concentration-dependent manner, as recently observed in rat brain (Gasull-Camos et al., 2017). The glutamate increase seen at the higher dose used in the present study (3 mM) was similar to that found in rat prefrontal cortex by the same concentration (Gasull-Camos et al., 2017). However, the glutamate increase was significantly greater in *Epm2b−/−*than in *Epm2b+/+* mice, which indicates a lesser ability of GLT-1 to remove glutamate from excitatory synapses in the *Epm2b−/−*mice (Fig. 5). Hence, although basal glutamate concentrations in the extracellular brain space are not representative of the neurotransmitter pool, certain pharmacological treatments, such as non-competitive NDMA-R antagonists (Moghaddam et al., 1997) or glutamate transporter inhibitors (Gasull-Camos et al., 2017) increase dialysate glutamate concentrations thus providing a reliable measure of the neurotransmitter pool and of the parallel increase in excitatory transmission (Fullana et al., 2019).

This view is also supported by the observation that PTZ elevated extracellular glutamate levels more in *Epm2b−/−* than in *Epm2b+/+* mice (Fig. 2B and 2C). Although genotype differences did not reach statistical significance when comparing individual levels in each dialysate fraction, they reached statistical significance when the overall effect (AUC values) were compared, at least for the smaller dose used (10 mg/kg) (Fig. 2C). The elevation of extracellular glutamate levels induced by PTZ is likely due to the blockade of GABA-mediated neurotransmission and the subsequent increase of the excitation/inhibition ratio, leading to an enhanced glutamate release by hippocampal excitatory synapses. The higher glutamate levels in *Epm2b−/−* mice are likely to be explained by the compromised GLT-1 function in these mice, resulting in a lower ability to remove synaptic glutamate.

In our opinion, the small differences we observed in terms of glutamate uptake (Fig. 2) could explain the weak phenotype of the *Epm2b−/−* mice in terms of seizures. In our hands, and in agreement with other authors, only if the *Epm2b−/−* mice are treated with PTZ, the appearance of seizures are clearly observed, showing these mice a higher sensitivity to this drug than control animals. However, our results clearly point to an in vivo dysregulation of glutamate uptake in *Epm2b−/−* mice, which correlates with our previous results on the decreased capacity of primary astrocytes to transport glutamate (Munoz-Ballester et al., 2016).

Since our results suggested a dysfunction in GLT-1 activity as the underlying cause of the impairment in glutamate clearance in the hippocampus of *Epm2b−/−* mice, we were interested in analyzing *Glt-1* expression levels in *Epm2b+/+* and *Epm2b−/−* mice. Since LD is a neurodegenerative disorder in which the patient's health declines with time, we decided to analyze the expression of *Glt-1* at different ages: in very young animals (16 days), mice of 3 months of age (at the beginning of the development of the pathophysiological phenotypes) and 12 months old animals, which present a florid pathophysiology (previous results in the lab indicated no major changes in the expression of genes between 9 and 12 months of age, indicating that after 9 months the molecular determinants of the disease are already present; in fact, animals from 9 to 13 months display similar pathophysiological phenotypes (Criado et al., 2012)). When we analyzed the mRNA levels of the two major *Glt-1* isoforms, *Glt-1a* and *Glt-1b*, we found an increase in *Glt-1b* expression at 12 months of age in the hippocampus of *Epm2b−/−* mice. This finding is interesting because a similar upregulation of *Glt-1b* expression has been also described in other neurological disorders, such as amyotrophic lateral sclerosis (ALS) (Maragakis et al., 2004), Parkinson (O'Donovan et al., 2015) and schizophrenia (McCullumsmith et al., 2016). This increase has been associated with a response to neurological stress (Maragakis et al., 2004), and it has been proposed that it could be a compensatory reaction to the loss of glial *Glt-1a* observed in ALS (Maragakis et al., 2004). Although we did not observe a decrease in *Glt-1a* expression in *Epm2b−/−* mice respect to control animals, the observed dysfunction in glutamate uptake could have triggered the increase in the expression of the *Glt-1b* isoform. However, the role that this upregulation could have in the maintenance of the glutamate homeostasis is still unknown. It is important to mention that GLT-1b isoform presents a differential C-terminal domain that is absent in GLT-1a which allows this isoform to interact with other proteins and regulate its intracellular trafficking ((Sheng and Sala, 2001), (Bassan et al., 2008)).

No changes in the expression of *Glast*, the other major glutamate transporter, were observed. However, we observed a decrease in *Eaac1* expression in *Epm2b−/−* at 12 months of age. Since EAAC1 is mainly expressed in neurons and LD is characterized by neurodegeneration, we interpret this result as a consequence of the neuronal loss characteristic of LD.

When we analyzed the total GLT-1 protein expression by immunostaining, we could not find any difference between *Epm2b+/+* and *Epm2b−/−* animals. These results were in agreement with previous results showing no differences in total GLT-1 protein levels in astrocytes from *Epm2a−/−* or *Epm2b−/−* animals (Munoz-Ballester et al., 2016). In that work we described a deficiency in the competence of astrocytes from LD models to uptake glutamate and suggested that this defect was due to a decreased localization of the transporter at the plasma membrane. This change in the subcellular localization of the transporter could impair glutamate transport and be responsible for the excess of extracellular glutamate detected *in vivo*. A possible explanation for the lack of correlation between the increase in mRNA expression of *Glt-1b* and no changes in total GLT-1 protein levels could be that the *Glt-1b* mRNA is less competent in translation, as suggested in (Sutherland et al., 1996).

CONCLUSIONS

In summary, we have identified a certain region of the hippocampus as an area of interest in LD due to increased neuronal activity. Furthermore, we have detected in this area an impairment in glutamate clearance in *Epm2b−/−* animals compared to *Epm2b+/+* mice. This suggests a dysregulation in the normal glutamate clearance by this transporter that could be contributing to an excess of excitation in this area, leading to epileptogenic events. Regarding the molecular basis of this process, we could not find any difference in the levels of the GLT-1 protein, but we found an important increase in the levels of *Glt-1b* mRNA, which has been associated previously with neuronal stress. With all these results, we propose that GLT-1 is a key element in the origin of epilepsy in LD. GLT-1 function would be decreased in the hippocampus of LD animals, leading to an excess of extracellular glutamate that could hyperactivate neurons in that area and favor epileptogenesis.

ACKNOWLEDGMENTS

This work was supported by grants from the Spanish Ministry of Economy and Competitiveness SAF2014–54604-C3–1-R, SAF2017–83151-R (to P.S.) and SAF2015–68346-P (to F.A.), co-funded by the European Regional Development Fund “A way to build Europe” (to F.A.), a grant from Fundación Ramón Areces (CIVP18A3935) and a grant from the National Institute of Health (NIH-NINDS) P01NS097197, which established the Lafora Epilepsy Cure Initiative (LECI), to PS. The Centro de Investigación Biomédica en Red de Salud Mental (CIBERSAM) and de Enfermedades Raras (CIBERER) are also acknowledged for financial support. We also thank Letizia Campa and Verónica Paz for their outstanding technical assistance.

REFERENCES

Aguado C, Sarkar S, Korolchuk VI, Criado O, Vernia S, Boya P, Sanz P, de Cordoba SR, Knecht E, Rubinsztein DC, 2010 Laforin, the most common protein mutated in Lafora disease, regulates autophagy. Hum Mol Genet 19, 2867–2876. [PubMed: 20453062]

Andre V, Pineau N, Motte JE, Marescaux C, Nehlig A, 1998 Mapping of neuronal networks underlying generalized seizures induced by increasing doses of pentylenetetrazol in the immature and adult rat: a c-Fos immunohistochemical study. Eur J Neurosci 10, 2094–2106. [PubMed: 9753096]

Arriza JL, Eliasof S, Kavanaugh MP, Amara SG, 1997 Excitatory amino acid transporter 5, a retinal glutamate transporter coupled to a chloride conductance. Proc Natl Acad Sci USA 94, 4155–4160. [PubMed: 9108121]

Arriza JL, Fairman WA, Wadiche JI, Murdoch GH, Kavanaugh MP, Amara SG, 1994 Functional comparisons of three glutamate transporter subtypes cloned from human motor cortex. J Neurosci 14, 5559–5569. [PubMed: 7521911]

Bassan M, Liu H, Madsen KL, Armsen W, Zhou J, Desilva T, Chen W, Paradise A, Brasch MA, Staudinger J, Gether U, Irwin N, Rosenberg PA, 2008 Interaction between the glutamate transporter GLT1b and the synaptic PDZ domain protein PICK1. Eur J Neurosci 27, 66–82. [PubMed: 18184314]

Brancaccio M, Edwards MD, Patton AP, Smyllie NJ, Chesham JE, Maywood ES, Hastings MH, 2019 Cell-autonomous clock of astrocytes drives circadian behavior in mammals. Science 363, 187–192. [PubMed: 30630934]

Calcagno E, Carli M, Invernizzi RW, 2006 The 5-HT(1A) receptor agonist 8-OH-DPAT prevents prefrontocortical glutamate and serotonin release in response to blockade of cortical NMDA receptors. J Neurochem 96, 853–860. [PubMed: 16405507]

Coulter DA, Eid T, 2012 Astrocytic regulation of glutamate homeostasis in epilepsy. Glia 60, 1215–1226. [PubMed: 22592998]

Criado O, Aguado C, Gayarre J, Duran-Trio L, Garcia-Cabrero AM, Vernia S, San Millan B, Heredia M, Roma-Mateo C, Mouron S, Juana-Lopez L, Dominguez M, Navarro C, Serratosa JM, Sanchez M, Sanz P, Bovolenta P, Knecht E, Rodriguez de Cordoba S, 2012 Lafora bodies and neurological defects in malin-deficient mice correlate with impaired autophagy. Hum Mol Genet 21, 1521–1533. [PubMed: 22186026]

Chan EM, Young EJ, Ianzano L, Munteanu I, Zhao X, Christopoulos CC, Avanzini G, Elia M, Ackerley CA, Jovic NJ, Bohlega S, Andermann E, Rouleau GA, Delgado-Escueta AV, Minassian BA, Scherer SW, 2003 Mutations in NHLRC1 cause progressive myoclonus epilepsy. Nat Genet 35, 125–127. [PubMed: 12958597]

Cho S, Muthukumar AK, Stork T, Coutinho-Budd JC, Freeman MR, 2018 Focal adhesion molecules regulate astrocyte morphology and glutamate transporters to suppress seizure-like behavior. Proc Natl Acad Sci USA 115, 11316–11321. [PubMed: 30327343]

Choi DW, Hartley DM, 1993 Calcium and glutamate-induced cortical neuronal death. Res Publ Assoc Res Nerv Ment Dis 71, 23–34. [PubMed: 8093332]

Danbolt NC, Furness DN, Zhou Y, 2016a Neuronal vs glial glutamate uptake: Resolving the conundrum. Neurochem Int 98, 29–45. [PubMed: 27235987]

Danbolt NC, Pines G, Kanner BI, 1990 Purification and reconstitution of the sodium-and potassium-coupled glutamate transport glycoprotein from rat brain. Biochemistry 29, 6734–6740. [PubMed: 1697765]

Danbolt NC, Storm-Mathisen J, Kanner BI, 1992 An [Na+ + K+]coupled L-glutamate transporter purified from rat brain is located in glial cell processes. Neuroscience 51, 295–310. [PubMed: 1465194]

Danbolt NC, Zhou Y, Furness DN, Holmseth S, 2016b Strategies for immunohistochemical protein localization using antibodies: What did we learn from neurotransmitter transporters in glial cells and neurons. Glia 64, 2045–2064. [PubMed: 27458697]

Dragunow M, Faull R, 1989 The use of c-fos as a metabolic marker in neuronal pathway tracing. J Neurosci Methods 29, 261–265. [PubMed: 2507830]

Fairman WA, Vandenberg RJ, Arriza JL, Kavanaugh MP, Amara SG, 1995 An excitatory amino-acid transporter with properties of a ligand-gated chloride channel. Nature 375, 599–603. [PubMed: 7791878]

Ferland RJ, Nierenberg J, Applegate CD, 1998 A role for the bilateral involvement of perirhinal cortex in generalized kindled seizure expression. Exp Neurol 151, 124–137. [PubMed: 9582260]

Franklin KBJ and Paxinos G, 2012 The mouse brain in stereotaxic coordinates, 4th edition ed. Academic Press, San Diego.

Fullana MN, Ruiz-Bronchal E, Ferres-Coy A, Juarez-Escoto E, Artigas F, Bortolozzi A, 2019 Regionally selective knockdown of astroglial glutamate transporters in infralimbic cortex induces a depressive phenotype in mice. Glia. In press.

Garcia-Cabrero AM, Sanchez-Elexpuru G, Serratosa JM, Sanchez MP, 2014 Enhanced sensitivity of laforin-and malin-deficient mice to the convulsant agent pentylenetetrazole. Front Neurosci 8, 291. [PubMed: 25309313]

Gasull-Camos J, Tarres-Gatius M, Artigas F, Castane A, 2017 Glial GLT-1 blockade in infralimbic cortex as a new strategy to evoke rapid antidepressant-like effects in rats. Transl Psychiatry 7, e1038. [PubMed: 28221365]

Herrera DG, Robertson HA, 1996 Activation of c-fos in the brain. Prog Neurobiol 50, 83–107. [PubMed: 8971979]

Hirsch E, Danober L, Simler S, Pereira de Vasconcelos A, Maton B, Nehlig A, Marescaux C, Vergnes M, 1997 The amygdala is critical for seizure propagation from brainstem to forebrain. Neuroscience 77, 975–984. [PubMed: 9130779]

Kadiyala SB, Papandrea D, Tuz K, Anderson TM, Jayakumar S, Herron BJ, Ferland RJ, 2015 Spatiotemporal differences in the c-fos pathway between C57BL/6J and DBA/2J mice following flurothyl-induced seizures: A dissociation of hippocampal Fos from seizure activity. Epilepsy Res 109, 183–196. [PubMed: 25524858]

Kanai Y, Hediger MA, 1992 Primary structure and functional characterization of a high-affinity glutamate transporter. Nature 360, 467–471. [PubMed: 1280334]

Kargieman L, Santana N, Mengod G, Celada P, Artigas F, 2007 Antipsychotic drugs reverse the disruption in prefrontal cortex function produced by NMDA receptor blockade with phencyclidine. Proc Natl Acad Sci USA 104, 14843–14848. [PubMed: 17785415]

Klein BD, Fu YH, Ptacek LJ, White HS, 2004 c-Fos immunohistochemical mapping of the audiogenic seizure network and tonotopic neuronal hyperexcitability in the inferior colliculus of the Frings mouse. Epilepsy Res 62, 13–25. [PubMed: 15519128]

Konkle AT, Bielajew C, 2004 Tracing the neuroanatomical profiles of reward pathways with markers of neuronal activation. Rev Neurosci 15, 383–414. [PubMed: 15656286]

Llado-Pelfort L, Santana N, Ghisi V, Artigas F, Celada P, 2012 5-HT1A receptor agonists enhance pyramidal cell firing in prefrontal cortex through a preferential action on GABA interneurons. Cereb Cortex 22, 1487–1497. [PubMed: 21893679]

Maragakis NJ, Dykes-Hoberg M, Rothstein JD, 2004 Altered expression of the glutamate transporter EAAT2b in neurological disease. Ann Neurol 55, 469–477. [PubMed: 15048885]

McCullumsmith RE, O’Donovan SM, Drummond JB, Benesh FS, Simmons M, Roberts R, Lauriat T, Haroutunian V, Meador-Woodruff JH, 2016 Cell-specific abnormalities of glutamate transporters in schizophrenia: sick astrocytes and compensating relay neurons? Mol Psychiatry 21, 823–830. [PubMed: 26416546]

Meldrum B, 1986 Excitatory amino acid antagonists as novel anticonvulsants. Adv Exp Med Biol 203, 321–329. [PubMed: 3024459]

Meldrum B, 1991 Excitotoxicity and epileptic brain damage. Epilepsy Res 10, 55–61. [PubMed: 1790773]

Minassian BA, Ianzano L, Meloche M, Andermann E, Rouleau GA, Delgado-Escueta AV, Scherer SW, 2000 Mutation spectrum and predicted function of laforin in Lafora’s progressive myoclonus epilepsy. Neurology 55, 341–346. [PubMed: 10932264]

Minassian BA, Lee JR, Herbrick JA, Huizenga J, Soder S, Mungall AJ, Dunham I, Gardner R, Fong CY, Carpenter S, Jardim L, Satishchandra P, Andermann E, Snead OC 3rd, Lopes-Cendes I, Tsui LC, Delgado-Escueta AV, Rouleau GA, Scherer SW, 1998 Mutations in a gene encoding a novel protein tyrosine phosphatase cause progressive myoclonus epilepsy. Nat Genet 20, 171–174. [PubMed: 9771710]

Moghaddam B, Adams B, Verma A, Daly D, 1997 Activation of glutamatergic neurotransmission by ketamine: a novel step in the pathway from NMDA receptor blockade to dopaminergic and cognitive disruptions associated with the prefrontal cortex. J Neurosci 17, 2921–2927. [PubMed: 9092613]

Munoz-Ballester C, Berthier A, Viana R, Sanz P, 2016 Homeostasis of the astrocytic glutamate transporter GLT-1 is altered in mouse models of Lafora disease. Biochim Biophys Acta 1862, 1074–1083. [PubMed: 26976331]

Murphy-Royal C, Dupuis J, Groc L, Oliet SHR, 2017 Astroglial glutamate transporters in the brain: Regulating neurotransmitter homeostasis and synaptic transmission. J Neurosci Res 95, 2140–2151. [PubMed: 28150867]

O'Donovan SM, Hasselfeld K, Bauer D, Simmons M, Roussos P, Haroutunian V, Meador-Woodruff JH, McCullumsmith RE, 2015 Glutamate transporter splice variant expression in an enriched pyramidal cell population in schizophrenia. Transl Psychiatry 5, e579. [PubMed: 26057049]

Oliveira JF, Sardinha VM, Guerra-Gomes S, Araque A, Sousa N, 2015 Do stars govern our actions? Astrocyte involvement in rodent behavior. Trends Neurosci 38, 535–549. [PubMed: 26316036]

Olney JW, Collins RC, Sloviter RS, 1986 Excitotoxic mechanisms of epileptic brain damage. Adv Neurol 44, 857–877. [PubMed: 3706027]

Olney JW, Sharpe LG, Feigin RD, 1972 Glutamate-induced brain damage in infant primates. J Neuropathol Exp Neurol 31, 464–488. [PubMed: 4626680]

Ortolano S, Vieitez I, Agis-Balboa RC, Spuch C, 2014 Loss of GABAergic cortical neurons underlies the neuropathology of Lafora disease. Mol Brain 7, 7. [PubMed: 24472629]

Perea G, Araque A, 2007 Astrocytes potentiate transmitter release at single hippocampal synapses. Science 317, 1083–1086. [PubMed: 17717185]

Perea G, Sur M, Araque A, 2014 Neuron-glia networks: integral gear of brain function. Front Cell Neurosci 8, 378. [PubMed: 25414643]

Petr GT, Sun Y, Frederick NM, Zhou Y, Dhamne SC, Hameed MQ, Miranda C, Bedoya EA, Fischer KD, Armsen W, Wang J, Danbolt NC, Rotenberg A, Aoki CJ, Rosenberg PA, 2015 Conditional deletion of the glutamate transporter GLT-1 reveals that astrocytic GLT-1 protects against fatal epilepsy while neuronal GLT-1 contributes significantly to glutamate uptake into synaptosomes. J Neurosci 35, 5187–5201. [PubMed: 25834045]

Robel S, Buckingham SC, Boni JL, Campbell SL, Danbolt NC, Riedemann T, Sutor B, Sontheimer H, 2015 Reactive astrogliosis causes the development of spontaneous seizures. J Neurosci 35, 3330–3345. [PubMed: 25716834]

Rubio-Villena C, Viana R, Bonet J, Garcia-Gimeno MA, Casado M, Heredia M, Sanz P, 2018 Astrocytes: new players in progressive myoclonus epilepsy of Lafora type. Hum Mol Genet 27, 1290–1300. [PubMed: 29408991]

Sagar SM, Sharp FR, Curran T, 1988 Expression of c-fos protein in brain: metabolic mapping at the cellular level. Science 240, 1328–1331. [PubMed: 3131879]

Santana N, Troyano-Rodriguez E, Mengod G, Celada P, Artigas F, 2011 Activation of thalamocortical networks by the N-methyl-D-aspartate receptor antagonist phencyclidine: reversal by clozapine. Biol Psychiatry 69, 918–927. [PubMed: 21251645]

Serratosa JM, Gomez-Garre P, Gallardo ME, Anta B, de Bernabe DB, Lindhout D, Augustijn PB, Tassinari CA, Malafosse RM, Topcu M, Grid D, Dravet C, Berkovic SF, de Cordoba SR, 1999 A novel protein tyrosine phosphatase gene is mutated in progressive myoclonus epilepsy of the Lafora type (EPM2). Hum Mol Genet 8, 345–352. [PubMed: 9931343]

Sharma J, Mukherjee D, Rao SN, Iyengar S, Shankar SK, Satishchandra P, Jana NR, 2013 Neuronatin-mediated aberrant calcium signaling and endoplasmic reticulum stress underlie neuropathology in Lafora disease. J Biol Chem 288, 9482–9490. [PubMed: 23408434]

Sheng M, Sala C, 2001 PDZ domains and the organization of supramolecular complexes. Annu Rev Neurosci 24, 1–29. [PubMed: 11283303]

Storck T, Schulte S, Hofmann K, Stoffel W, 1992 Structure, expression, and functional analysis of a Na(+)-dependent glutamate/aspartate transporter from rat brain. Proc Natl Acad Sci USA 89, 10955–10959. [PubMed: 1279699]

Sutherland ML, Delaney TA, Noebels JL, 1996 Glutamate transporter mRNA expression in proliferative zones of the developing and adult murine CNS. J Neurosci 16, 2191–2207. [PubMed: 8601800]

Tanaka K, Watase K, Manabe T, Yamada K, Watanabe M, Takahashi K, Iwama H, Nishikawa T, Ichihara N, Kikuchi T, Okuyama S, Kawashima N, Hori S, Takimoto M, Wada K, 1997 Epilepsy and exacerbation of brain injury in mice lacking the glutamate transporter GLT-1. Science 276, 1699–1702. [PubMed: 9180080]

Turnbull J, Tiberia E, Striano P, Genton P, Carpenter S, Ackerley CA, Minassian BA, 2016 Lafora disease. Epileptic Disord 18, 38–62. [PubMed: 27702709]

Author Manuscript

Author Manuscript

Author Manuscript

Highlights:

- Lafora disease mouse model shows increased neuronal activity in the hippocampus.
- This area presented lesser ability to remove synaptic glutamate.
- There is an increased expression of the Glt-1b isoform related to neuronal stress.
- Dysregulation of glutamate clearance could contribute to epileptogenesis in LD.

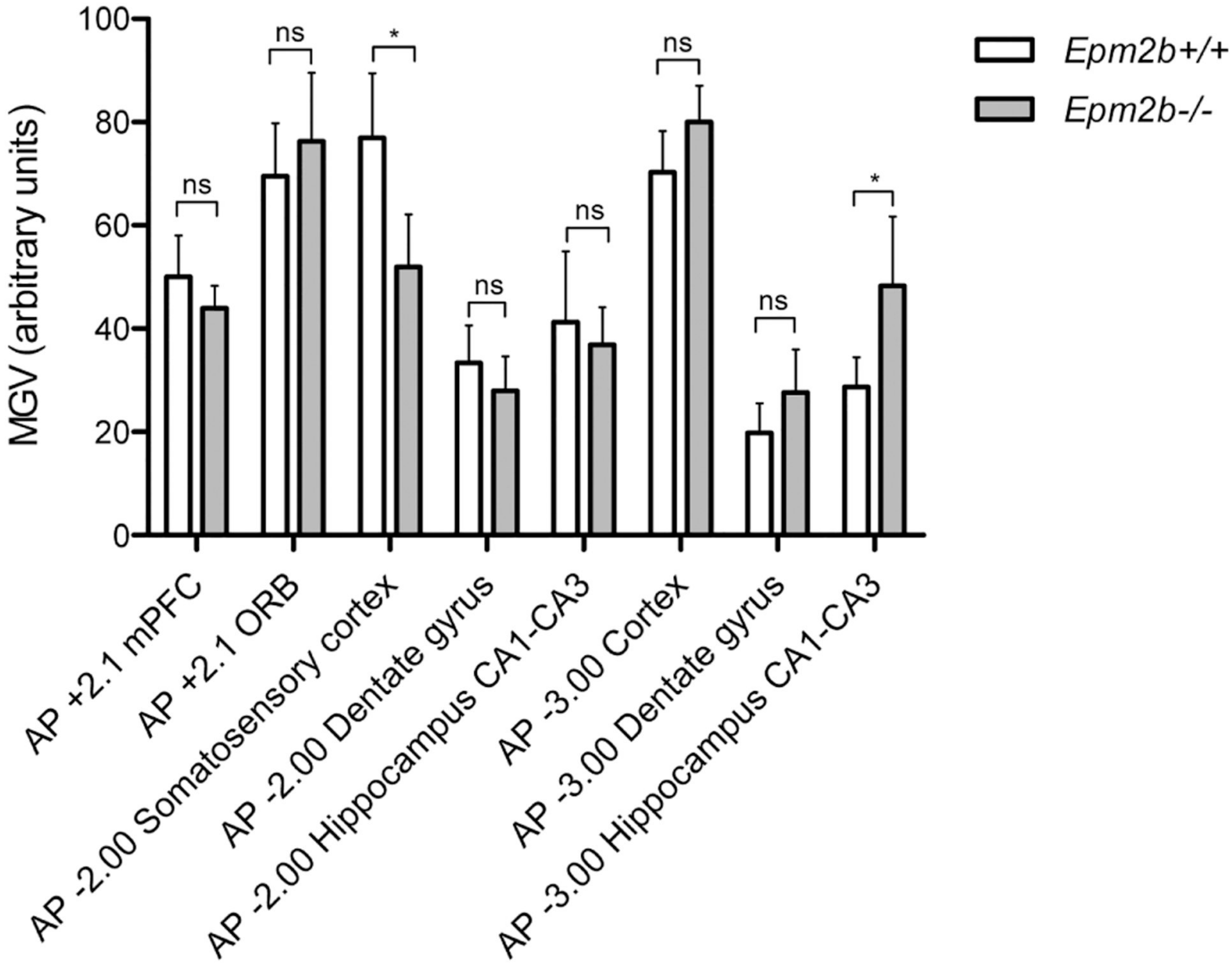

Figure 1. c-*fos* expression in *Epm2b*+/+ and *Epm2b*−/− brain areas detected by *in situ* hybridization.

Bar graph shows the optical density (mean grey value, MGV) of c-*fos* mRNA signal in each area of the brain for each genotype analyzed by *in situ* hybridization (n=4). AP = anterio-posterior axis, PFC = prefrontal cortex, ORB = orbital cortex, CA = cornus ammonis. The asterisk indicates a p-value<0.05 comparing *Epm2b+/+* and *Epm2b−/−* (Student's *t*-test); ns, not statistically significant.

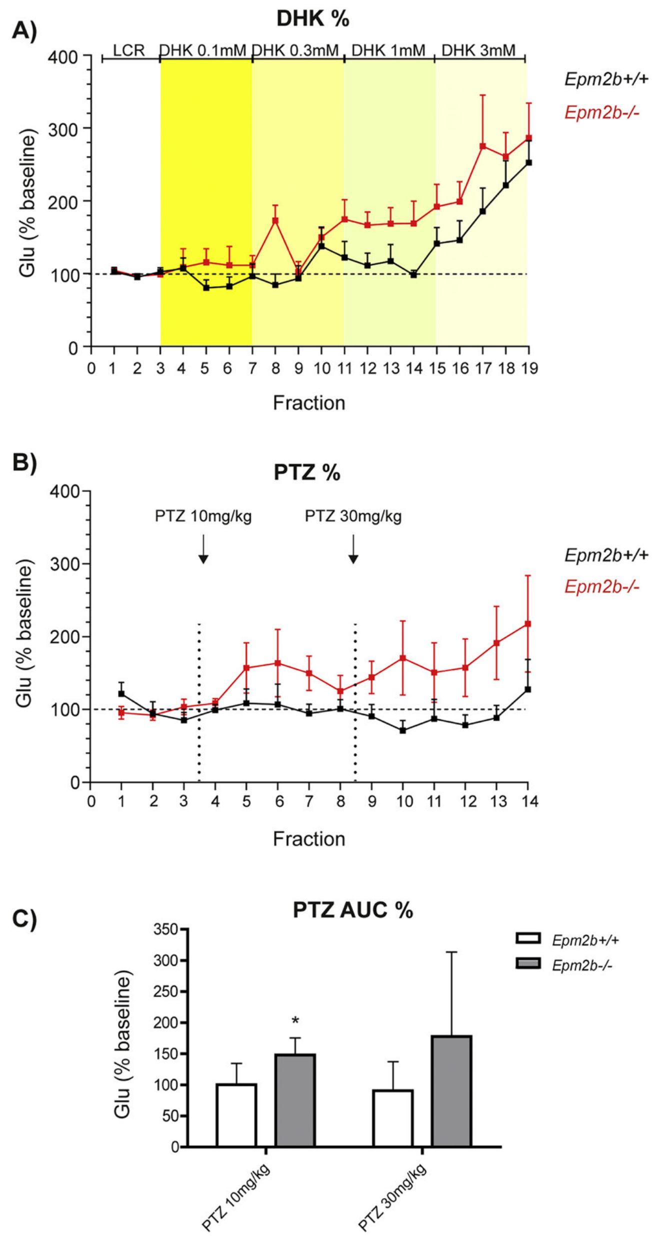

Figure 2. Extracellular glutamate levels in the hippocampus of *Epm2b*+/+ and *Epm2b*−/− after DHK and PTZ administration.

A) Effect of the GLT-1 inhibitor dihydrokainate (DHK) on hippocampal extracellular levels of glutamate in *Epm2b+/+ and Epm2b−/−* mice. DHK was applied by reverse dialysis at increasing nominal concentrations (0.1, 0.3, 1 and 3 mM, four consecutive fractions each). Yellow stripes represent the different concentrations of DHK administered locally. Black and red lines correspond, respectively, to *Epm2b+/+ and Epm2b−/−* animals. Data (mean +/− SD) from 7 *Epm2b+/+* animals and 8 *Epm2b−/−* mice were expressed as percentages of individual basal values. Higher levels of glutamate were detected in *Epm2b−/−* mice ($p<0.05$, two-way ANOVA, Bonferroni post-hoc test). B and C) Effect of the pro-convulsive agent pentilenetetrazol (PTZ) on extracellular glutamate levels in mouse hippocampus. B) The dialysate data is expressed as percentages of individual basal values, as in A). Black and red lines correspond, respectively, to *Epm2b+/+ and Epm2b−/−* animals. Arrows mark the time of injection of the different doses of PTZ (10 mg/kg and 30 mg/kg). C) The Area Under the Curve (AUC) of dialysate fractions corresponding to each dose used (10 and 30 mg/kg, respectively) is shown. AUC values revealed a greater effect of PTZ in increasing glutamate levels in *Epm2b−/−* mice (*$p<0.05$, multiple *t*-test) at the 10 mg/kg dose. Glu: glutamate

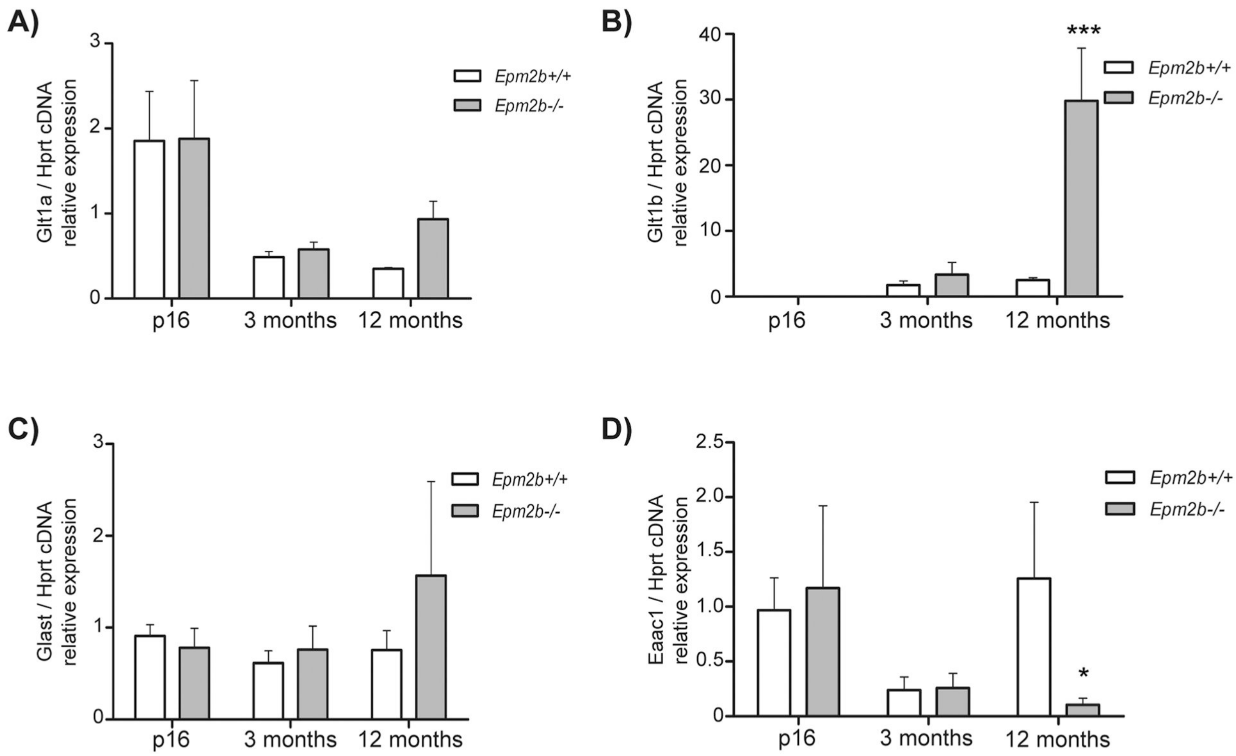

Figure 3. qPCR analysis of *Glt-1a*, *Glt-1b*, *Glast* and *Eaac1* in hippocampus of *Epm2b+/+* and *Epm2b−/−* mice.

Glt-1a/*Hprt* (A), *Glt-1b/Hprt* (B), *Glast/Hprt* (C) and *Eaac1/Hprt* (D) relative cDNA expression levels in *Epm2b+/+* and *Epm2b−/−* animals at p16, 3 months and 12 months of age. In A), no statistical difference was found between groups (two-way ANOVA, Bonferroni test post-hoc, n=3). In B), at 12 months of age, *Epm2b−/−* mice express more *Glt1-b* than *Epm2b+/+* (p-value ***<0.001, n= 3; two-way ANOVA, Bonferroni test post-hoc). In C), no statistical difference was found between groups (n= 3; two-way ANOVA, Bonferroni test post-hoc). In D), at 12 months of age, *Epm2b−/−* mice express less *Eaac1* than *Epm2b+/+* (p-value *<0.05, n= 3; two-way ANOVA, Bonferroni test post-hoc).

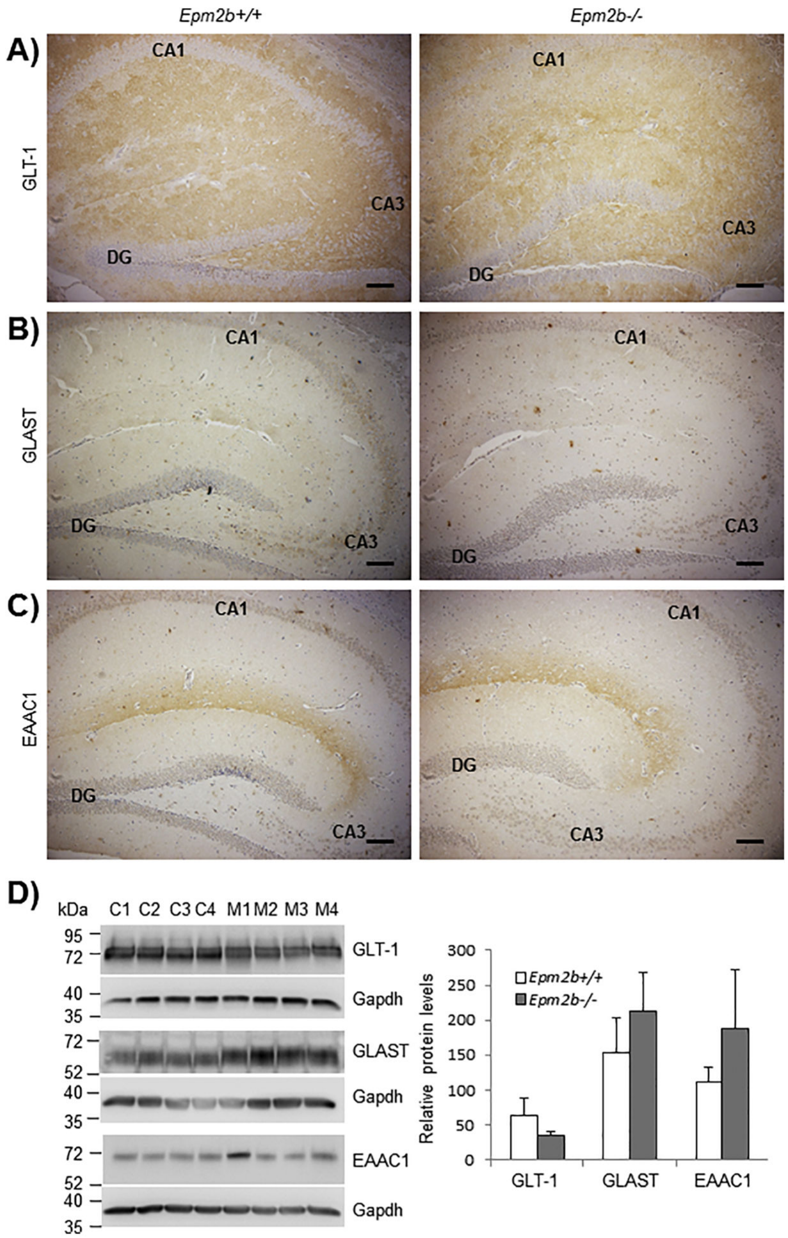

Figure 4. Immunohistochemistry analyses of GLT-1, GLAST and EAAC1 in the hippocampus of 12-month-old *Epm2b*+/+ and *Epm2b*−/− mice.

Antibodies against GLT-1 (A), GLAST (B) and EAAC1 (C) were used. Brown staining labels the presence of the protein of interest by ABC detection (see Materials and Methods). No differences in staining between *Epm2b−/−* and *Epm2b+/+* samples were observed. The position of the dentate girus (DG) cornus ammonis 1 (CA1) and cornus ammonis 3 (CA3) in the hippocampus is indicated in each case. Scale bar: 100 μm. D) Western blot analyses of hippocampal samples from *Epm2b+/+* and *Epm2b−/−* mice. In the left panel, crude extracts (10 μg protein to detect GLT-1 and 25 μg protein to detect GLAST and EAAC1) were analyzed using the corresponding antibodies in four independent samples from *Epm2b+/+* (C1–C4) and *Epm2b−/−* (M1–M4) mice. The levels of Gapdh were used as loading control.

Molecular weight markers are indicated in the left. In the right panel, relative intensity of the bands respect to Gapdh was plotted. No statistical differences were observed (Student *t*-test).

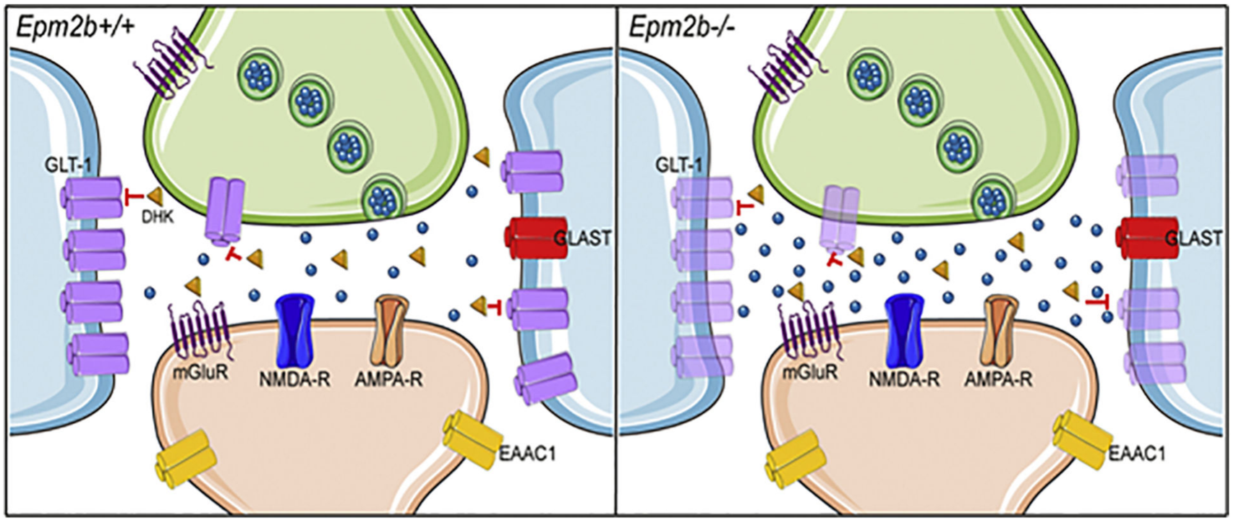

Figure 5. Lafora disease mouse model accumulates higher amounts of glutamate at the synaptic space.

Schematic view of hippocampal glutamatergic tripartite synapse in control (*Epm2b+/+*) and *Epm2b−/−* mice. Presynaptic neuron is colored in green, postsynaptic neuron is colored in light orange, astrocytes are colored in blue. The main cellular localization of different glutamate transporters (GLT-1, GLAST, EAAC1) and glutamate receptors (mGluR, NMDA-R, AMPA-R) is also indicated. Glutamate molecules are shown as blue spheres and dihydrokainate (DHK) as orange triangles. The blockade of GLT-1 by DHK (red lines) evoked a greater elevation of extracellular glutamate in *Epm2b−/−* mice than in control mice. This effect if possibly associated to the upregulation of the minor isoform of the *Glt-1* gene (*Glt-1b*), which is pictured in pale magenta. This figure was created using Server Medical Art templates, which are licensed under Creative Commons 3.0 Unported License: https://smart.servier.com.

Table I.

Sequence of the primers used for qPCR analyses of the corresponding genes. The probe number according to the Roche ProbeFinder software is also indicated.

Gene of interest	Forward primer	Reverse primer	Probe number
Glt-1a	GATGCCTTCCTGGATCTCATT	CAGAACTTTCTTTGTCACTGTCTGA	103
Glt-1b	TTCTACAGCTGAGAGAATGGTCA	TTCGGTGCTTTGGCTCAT	83
Glast	AGAAGGTAAAATCGTGCAGGTC	ACCAGATTGGGAGGGAACT	84
Eaac1	TTTTCCTGGGGAAATTCTGA	ATCCAGTGCAGCGACACC	89
Hprt	TCCTCCTCAGACCGACTTTT	CCTGGTTCATCATCGCTAATC	95